Isothermal calorimetry tests and modeling of cement hydration parameters

Qinwu Xu [a], Jiong Hu [b],[*], J. Mauricio Ruiz [a], Kejin Wang [c], Zhi Ge [d]

[a] *The Transtec Group Inc., 6111 Balcones Dr., Austin, TX 78731, USA*
[b] *Department of Engineering Technology, Texas State University - San Marcos, 1244 RFM, 601 University Drive, San Marcos, TX 78666, USA*
[c] *Department of Civil, Construction, and Environmental Engineering, Iowa State University, 492 Town Engineering Building, Ames, IA 50011, USA*
[d] *Department of Transportation Engineering, Shandong University, Jinshilu 73, Jinan, Shandong 250061, China*

ABSTRACT

Degree of cement hydration can be characterized by hydration parameters including activation energy (E_a) and hydration curve parameters (ultimate hydration degree α_u, hydration shape parameter β, and hydration time parameter τ). These parameters are affected by material compositions including chemical and mineral admixtures. In this study, isothermal calorimetry tests were performed at different ambient temperatures with cement mortar mixtures with different amounts of water reducers and fly ashes. Hydration model was used to back-calculate hydration parameters using the measured heat generation–time relationship. Results showed that the activation energy E_a generally increases with increasing water reducer dosage and fly ash replacement. Hydration curve parameter α_u seems to decreases, while τ generally increases with increasing water reducer dosage and fly ash replacement, and β seems to increase with increasing water reducer dosage. As a result, the simulated temperature developments in the early-age concrete pavement showed that increased water reducer dosage and fly ash replacement results in decreased pavement temperature, thus reduced thermally-induced stress.

© 2009 Elsevier B.V. All rights reserved.

1. Introduction

Temperature development in the early-age concrete plays an important role in the developments of material properties and performances such as hardening [1], critical stresses [2], and distresses [3]. While heat is evolved with cement hydration due to the breaking and making of chemical bonds during cement hydration, the strength of concrete is very much dependent upon the hydration reaction as well. For this reason, the concrete strength development is generally considered to be directly related to heat of hydration. The same mechanism can also be applied to develop maturity meters to predict concrete strength at different ages based on the monitoring of hydration heat [3,4]. It is also a well known fact that the portland cement concrete pavement (PCCP) will expand/contract or curl under temperature rise/decrease or temperature gradient [5,6]. Depends on the restrain condition and critical stress level inside the concrete pavement, the temperature gradient can result in distress or cracking as shown in Fig. 1. Cement hydration is the key element that affects the temperature development of early-age concrete due to the heat generation [7]. Therefore, it is essential to evaluate the hydration characteristics of concrete in order to capture the temperature development, so as to provide reliable material design and construction control.

The hydration characteristics can be evaluated by a group of hydration parameters including the activation energy and hydration curve parameters. Calorimetric tests, including isothermal, semi-adiabatic and fully adiabatic tests, are usually used to capture these hydration parameters.

The hydration characteristics and temperature developments in concrete are dependent of material compositions and mixture designs including additives such as cement, supplemental cementitious materials (SCMs), chemical admixtures, and polymers [8,9]. While water reducer (WR) is commonly used to reduce water contents and to improve concrete workability or strength, fly ash (FA) is also extensively used in modern concrete to replace a portion of portland cement so as to improve the engineering properties of concrete and reduce costs. Researches were conducted to study the effect of chemical admixtures and SCMs such as WR and FA in cement hydration. Results showed that with the increase of FA replacement, the hydration of the total cementitious system is retarded and the ultimate degree of hydration is increased, while the rate of hydration reaction is usually unaffected [10]. As the hydration of cement is a complex process involving multi-component solution, chemical reactions, decomposition and crystallization, the effect of chemical admixtures such as water reducer on cement hydration process is yet more complicate owing to the wide variety of them. Results showed that WR can increase
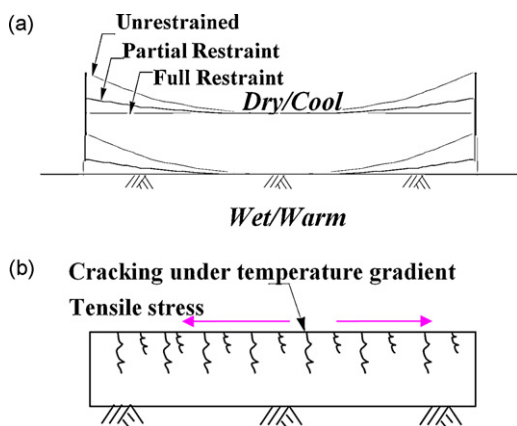
Fig. 1. Curling and distress development in PCCP.

the dispersivity of the cement particles and affect the rate of hydration of cement significantly [11]. On the other hand, various type of commercially available WR, especially those also act as retarder, can delay the hydration process because of the change of electrical behavior during hydration [12]. Therefore, a systematic study is needed to better justify the effect of WR and FA on the hydration process and thermal parameters.

The primary objective of this paper is to study the hydration characteristics of concrete containing FA and WR from calorimetric measurements. Isothermal calorimetry tests will be used to evaluate hydration characteristics of mixtures containing different amounts of WR and FA. The analytical hydration models will also be used to capture the hydration characteristics. Temperature and critical stress developments in the early-age PCCP are to be predicted based on the characterized hydration properties.

2. Experimental work

2.1. Raw materials and mix design

Three portland cement concrete pavement (PCCP) construction sites in the United States, i.e. Site A (Atlantic, Iowa), Site B (Alma Center, Wisconsin), and Site C (Ottumwa, Iowa), were included in the present study. The PCCP has a thickness of 20.3 cm (8 in.) for the Site A, while a thickness of 30.5 cm (12 in.) for Site B and Site C. The PCCP slab width is 4.88 m (16 ft), and slab length is 5.49 m (18 ft) in all three sites. Type IP (F), Type I/II GU, Type ISM cement were used in Site A, Site B, and Site C, respectively. Class C fly ashes (FA) were used in all three sites. The oxide compositions of cements and fly ashes used were measured using the X-ray fluorescence (XRF) method, with results summarized in Table 1. Air entraining agents (AEA) and water reducers were both used in all three sites. Noted that the water reducers used in the three sites were all lignosulfonate-based water reducers, and they are all Type D admixtures according to ASTM C 494 "*Standard specification for chemical admixtures for concrete*", which means that they also serve as retarder as they reduce the amount of required water. With materials collected from each of the three sites, nine mixtures of concrete and cement mortar as shown in Tables 2 and 3 with different WR dosages and FA replacement ratios were used in present study. The No.1 (normal) mixtures are the control mixes used in the field construction sites of the PCCP. Another eight mixtures contain various amounts of WR additives and/or FA replacements were prepared to study their influences on the hydration characteristics.

2.2. Experimental method

In present study, an isothermal calorimeter as shown in Fig. 2 was used to measure the heat generation of mortars with different mix designs at the National Concrete Pavement Technology (CP Tech) Center at the Iowa State University. In order to control the test condition, the isothermal calorimeter was placed in a temperature control chamber. The isothermal calorimeter contains eight separate channels, or units, each hold a single specimen during a test. As illustrated in the figure, each unit has an aluminum sample holder, which rests on a heat flow sensor (peltier) that is placed on a common heat sink of a large block of aluminum. On the other side of the heat sink is another heat flow sensor and a piece of 129-g aluminum block. The aluminum block is used as a reference to reduce the noise signal in this conduction calorimeter. When a sample is placed in the unit, the heat produced by hydration flows rapidly to its surroundings. The main route for heat exchange between the sample and the surroundings is through the heat flow detector. The heat flow, caused by the temperature difference across the sensor, creates a voltage signal proportional to the amount of heat flow. This voltage signal was then converted to the rate of heat evolution by applying the calibration factor based on the reference material (aluminum).

In order to investigate the effect of environmental temperature on cement heat of hydration, three different temperatures (20, 30, and 40 °C) were selected for the calorimetry tests. To control the concrete and mortar placement temperature, raw materials from the three sites were first stored in refrigerator, oven, or room condition prior to mixing. Mortars were then mixed according to ASTM C305 "*Standard practice for mechanical mixing of hydraulic cement pastes and mortars for plastic consistency*." Four specimens, with weights of 100 ± 2 g each, were placed into standard plastic containers and then loaded into the isothermal calorimeter as shown in Fig. 2 immediately after samples were ready. The produced heat was then conducted from the sample to the heat sink, and the temperature gradient across the heat detector produced a voltage proportional to the heat flow. After the samples were placed into the calorimeter, the pre-programmed calorimeter started taking readings immediately. The readings were taken every 30 s for a period of 48, or 24 h, depending upon the testing temperature. The rates of heat evolution per gram of cement were then calculated from the mix design of mortar mixtures, and the average values from four samples of each mix were used for analysis. A total of 81 mixtures were tested with isothermal calorimeter at three different temperatures.

Table 1
Oxide composition of cement and fly ash.

	Site A		Site B		Site C	
	Cement	Fly ash	Cement	Fly ash	Cement	Fly ash
CaO	49.34	26.20	63.09	25.60	58.79	28.80
SiO_2	29.64	34.90	20.78	36.30	23.72	31.60
Al_2O_3	8.20	20.10	4.74	19.10	5.22	16.20
Fe_2O_3	3.31	5.78	3.15	5.26	2.77	6.03
Na_2O	0.30	1.72	0.07	1.83	0.16	3.21
K_2O	0.73	0.42	0.78	0.47	0.56	0.32
MgO	3.08	4.63	2.35	5.29	4.30	6.81
SO_3	3.30	2.27	2.75	1.93	2.95	3.13
P_2O_5	0.10	1.01	0.08	1.03	0.10	1.02
TiO_2	0.51	1.64	0.24	1.53	0.38	1.24
SrO	0.12	0.42	0.11	0.44	0.04	0.51
Mn_2O_3	0.07	0.05	0.07	0.03	0.49	0.02
LOI[a]	1.29	0.38	1.78	0.36	0.51	0.30

[a] LOI: loss of ignition.

Table 2
Concrete mix designs.

Mixture no.	Cement (kg/m³)	Fly ash (kg/m³)	Coarse aggregate (kg/m³)	Intermedium aggregate (kg/m³)	Fine aggregate (kg/m³)	Water (kg/m³)	AEA (ml/100 kg)	WR (ml/100 kg)
Site A								
No.1: normal	262	65	926	162	777	131	20	261
No.2: +50% WR	262	65	926	162	777	131	20	391
No.3: −50% WR	262	65	926	162	777	131	20	130
No.4: +50% FA	230	98	926	162	777	131	20	261
No.5: −50% FA	295	33	926	162	777	131	20	261
No.6: +50% WR +50% FA	230	98	926	162	777	131	20	391
No.7: +50% WR −50% FA	295	33	926	162	777	131	20	391
No.8: −50% WR +50% FA	230	98	926	162	777	131	20	130
No.9: −50% WR −50% FA	295	33	926	162	777	131	20	130
Site B								
No.1: normal	265	67	1083	0	813	149	65	209
No.2: +50% WR	265	67	1083	0	813	149	65	313
No.3: −50% WR	265	67	1083	0	813	149	65	104
No.4: +50% FA	231	101	1083	0	813	149	65	209
No.5: −50% FA	298	34	1083	0	813	149	65	209
No.6: +50% WR +50% FA	231	101	1083	0	813	149	65	313
No.7: +50% WR −50% FA	298	34	1083	0	813	149	65	313
No.8:−50% WR +50% FA	231	101	1083	0	813	149	65	104
No.9: −50% WR −50% FA	298	34	1083	0	813	149	65	104
Site C								
No.1: normal	263	66	1095	0	766	132	20	261
No.2: +50% WR	263	66	1095	0	766	132	20	391
No.3: −50% WR	263	66	1095	0	766	132	20	130
No.4: +50% FA	230	99	1095	0	766	132	20	261
No.5: −50% FA	296	33	1095	0	766	132	20	261
No.6: +50% WR +50% FA	230	99	1095	0	766	132	20	391
No.7: +50% WR −50% FA	296	33	1095	0	766	132	20	391
No.8: −50% WR +50% FA	230	99	1095	0	766	132	20	130
No.9: −50% WR −50% FA	296	33	1095	0	766	132	20	130

Table 3
Mortar mix designs.

| Mixture no.	Sand/binder[a]	Water/binder	AEA (ml/100 kg binder)	Fly ash % (%binder)	WR (ml/100 kg binder)
Site A					
No.1: normal				20	261
No.2: +50% WR				20	391
No.3: −50% WR				20	130
No.4: +50% FA				30	261
No.5: −50% FA	2.37	0.40	20	10	261
No.6: +50% WR +50% FA				30	391
No.7: +50% WR −50% FA				10	391
No.8: −50% WR +50% FA				30	130
No.9: −50% WR −50% FA				10	130
Site B					
No.1: normal				20	209
No.2: +50% WR				20	313
No.3: −50% WR				20	104
No.4: +50% FA				30	209
No.5: −50% FA	2.45	0.45	65	10	209
No.6: +50% WR +50% FA				30	313
No.7: +50% WR −50% FA				10	313
No.8: −50% WR +50% FA				30	104
No.9: −50% WR −50% FA				10	104
Site C					
No.1: normal				20	261
No.2: +50% WR				20	391
No.3: −50% WR				20	130
No.4: +50% FA				30	261
No.5: −50% FA	2.33	0.40	20	10	261
No.6: +50% WR +50% FA				30	391
No.7: +50% WR −50% FA				10	391
No.8: −50% WR +50% FA				30	130
No.9: −50% WR −50% FA				10	130

[a] Binder = cement + fly ash.
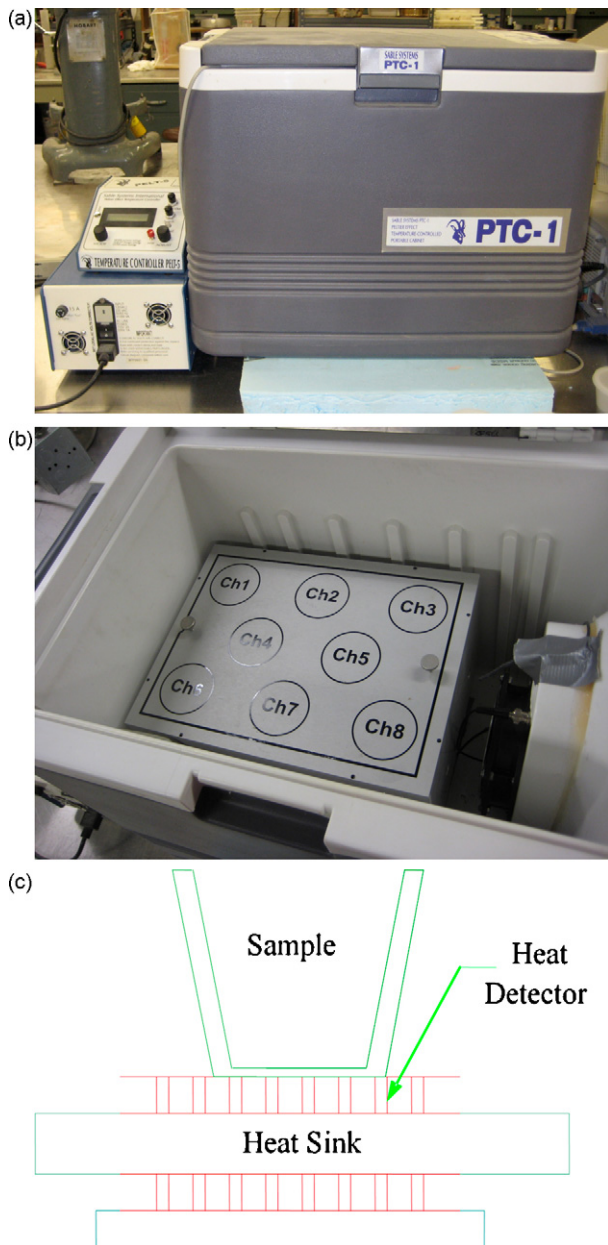
Fig. 2. Isothermal test device.

3. Hydration parameters and pavement temperature and stress prediction

3.1. Activation energy

Activation energy (E_a) is the minimum amount of energy required for a material to undergo a chemical reaction. Portland cement's activation energy is a critical material parameter in evaluating its hydration characteristics. The incremental method and the linear approximation methods as described in ASTM C 1074 "*Standard practice for estimating concrete strength by the maturity method*," can be used to compute E_a of different mixtures [13]. In this study, E_a was computed based on the Arrhenius equation [14] and isothermal test data as explained in the following.

Arrhenius equation, a formula accounts for the rate of temperature-dependent chemical reaction (referred as the rate of

heat generation, $P(T)$, in this paper), is defined as follows:

$$P(T) = Ae^{-E_a/RT}. \tag{1}$$

where A is the pre-exponential factor, T is temperature (K), and R is universal gas constant (8.3144 J/mol/°C).

A natural-logarithmic scale can then be applied on both sides of Eq. (1):

$$Ln[P(T)] = Ln(A) - \left(\frac{E_a}{R}\right)\frac{1}{T} \tag{2}$$

Eq. (2) shows that $Ln[P(T)]$ follows a linear function with $1/T$ (1/K). Thus, E_a (J/mol) can be determined from the slope of this linear function:

$$E_a = RT \cdot Log\frac{P(T)}{A} \tag{3}$$

The slope of this linear function ($-E_a/R$), can be obtained from the isothermal test results of $P(T)$ versus T.

3.2. Hydration curve parameters

Degree of hydration (DOH) of cementitious material at a specific time point t can be determined in terms of the generated heat and the total heat of cements [15]:

$$\alpha(t) = \frac{Q(t)}{H_u} \tag{4}$$

where $Q(t)$ is the accumulated generated heat at the time t during the hydration procedure, H_u is the total heat of a specific cementitious material that can be determined according to material components and chemical compositions [15].

The time t is usually converted to an equivalent age that expresses the maturity of cementitious material during its hardening procedure. The well-known equivalent age formula [16] is adopted in this research:

$$t_e = \sum \Delta t_e(T_r) = \sum e^{-E_a/R(1/T_c - 1/T_r)} \cdot \Delta t \tag{5}$$

where T_c is temperature (K), T_r is reference temperature (K), E_a is activation energy discussed above, and R is universal gas constant (8.3144 J/mol/°C).

Consequently, the degree of hydration is achieved using the following formula [13,14]:

$$\alpha(t_e) = \alpha_u \cdot \exp\left(-\left[\frac{\tau}{t_e}\right]^\beta\right) \tag{6}$$

where, $\alpha(t_e)$ is the degree of hydration at equivalent age, t_e is equivalent age at reference temperature of 21.1 °C (h), α_u is ultimate degree of hydration, τ is hydration time parameter (h), and β is hydration shape parameter.

α_u, τ, and β are the three hydration curve parameters used to characterize DOH of cementitious materials. A larger α_u indicates a higher magnitude of ultimate DOH, and a larger τ implies a larger delay of hydration. Since β represents the slope of the major linear part of the hydration shape, a larger β implies a higher hydration rate at the linear portion of hydration curves [14]. These three hydration curve parameters can be determined through the curve fitting and back-calculation by comparing DOHs determined from Eq. (6) with that determined from Eq. (4) in terms of the isothermal test data. Solver function embedded in the Microsoft Excel was used to optimize curving fitting procedure, and to obtain the three hydration curve parameters.

3.3. Pavement temperature and critical stress prediction

The temperatures and critical stresses of the PCCP are predicted using the Federal Highway Administration (FHWA) HIPERPAV®

software with the characterized hydration parameters as inputs parameters. HIPERPAV® is a validated engineering software used by state Departments of Transportations (DOTs), contractors of design and construction agencies to predict the early-age concrete and pavement behaviors including temperatures, critical stresses and strengths. The models for the temperature and stress predications, and their validations are detailed by previous researchers [17,18] and not discussed here.

By inputting the environmental weather information, construction conditions, and materials design parameters, HIPERPAV® was used to predict temperature developments in the first 72 h. In this paper, the local weather conditions were achieved from the Weather Underground Station. In order to study the effects of the FA and WR on the temperature developments, the nine dif-

ferent concrete mixture designs in each of the three sites were used as inputs for simulating temperature and stress developments of PCCP.

4. Results and analysis

4.1. Heat generation

The isothermal test results of heat generation rates (mV/g) of all these nine different mixtures from materials collected from each of the three field sites were illustrated in Figs. 3–5. Results showed that the mixes with additional WR and FA are mostly "shifted" to the right side of the normal mix, while the mixes with reduced WR and
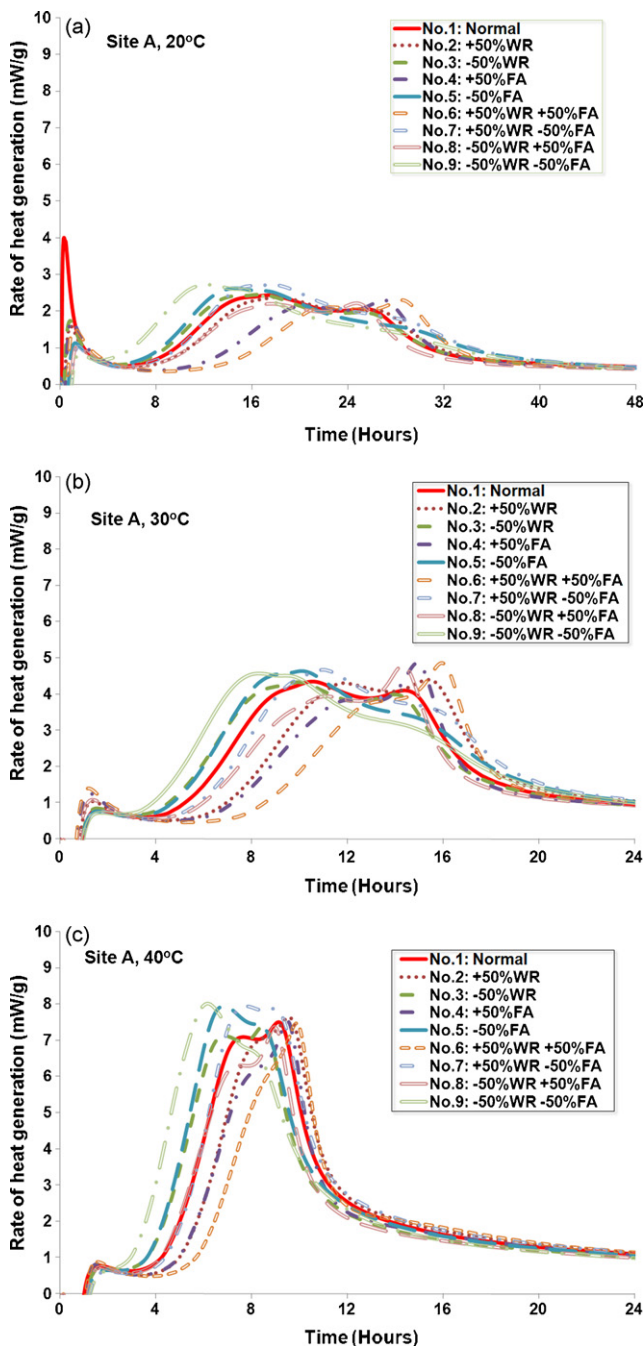

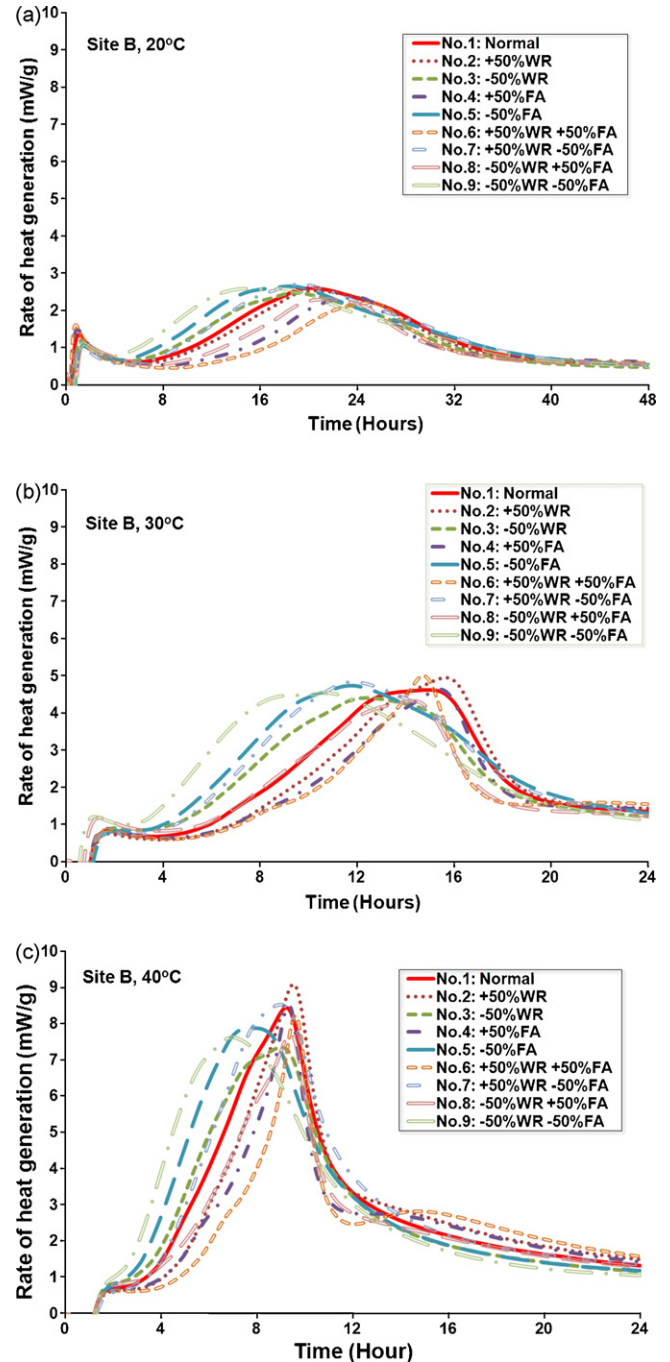**Fig. 3.** Isothermal test results from Site A mortar mixes at different temperatures.

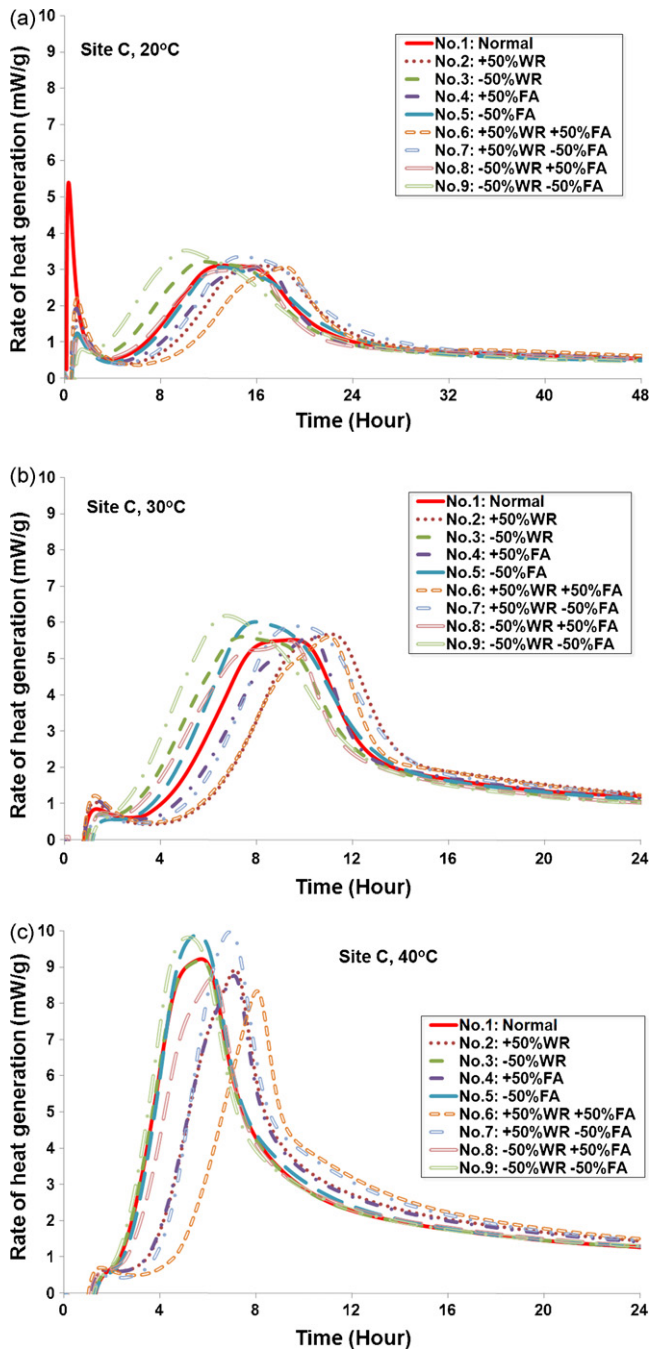**Fig. 4.** Isothermal test results from Site B mortar mixes at different temperatures.

Fig. 5. Isothermal test results from Site C mortar mixes at different temperatures.

FA are mostly "shifted" to the left, indicating the retarding effect of WR and FA on the hydration. Meanwhile, results showed that heat generation "accelerates" with the increasing temperature, i.e., the heat generation rate is higher with higher temperature at the same time point. The maximum rate of heat generation and the area under the major peaks was found to increase with increased temperature, while the time to reach this maximum rate decreased. The results from present study indicated that high curing temperature is favorable to the concrete strength development, and extended curing time is needed for the concrete to gain a specific strength value when concrete is under a low temperature environmental condition. It should be noted that although isothermal test results from all three field sites presented a second peaks, the double peaks pattern is more noticeable in Site A mixes comparing to the mixes from other sites. This phenomenon is likely due to the fact that a
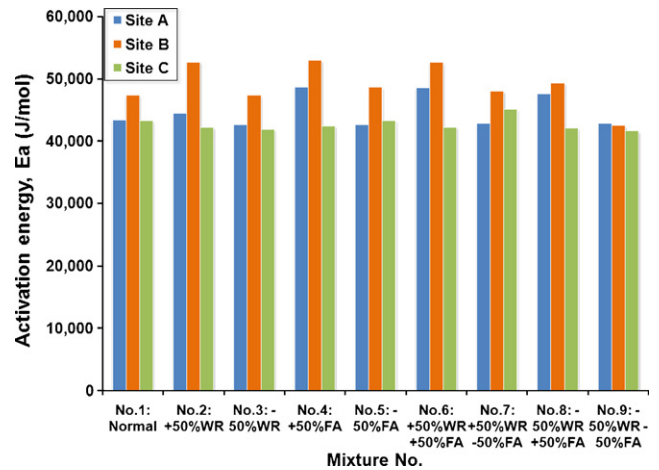

Fig. 6. Calculated activation energies (E_a) from isothermal tests.

much lower CaO content was found in the cement used in Site A, which indicated that a higher percentage of SCMs was used in the cement. The phenomenon is consistent with founding from other researchers that a high percentage of SCMs replacement can generally result in another delayed hydration peak due to the slower pozzolans reaction [19,20].

4.2. Activation energy

As shown in Fig. 6, the calculated activation energies E_a from isothermal tests were found to be ranged from 41,581 to 52,664 J/mol. These values are close to those reported by other researchers, e.g. Tank [21] reported that E_a ranges from 30,000 to 62,000 J/mol, Wadsö [15] reported that E_a ranges from 33,500 to 41,000 J/mol.

Results showed that mixtures of Site B generally have the highest E_a, comparing to mixtures of Site A, and Site C, which is probably due to the difference of cements and fly ashes used in different sites (see Table 1). It seems that mostly E_a increases with increasing WR and/or FA replacement (e.g. E_a increases 11.14%, 11.73%, and 11.00% for mixtures of No.2, No.4, and No.6, respectively, compared to the controlled mixture of No.1). Within all the mixes, mixture No.9 has the lowest E_a. The results are consistent with observation from previous researchers that the activation energy E_a increases with increasing FA [14].
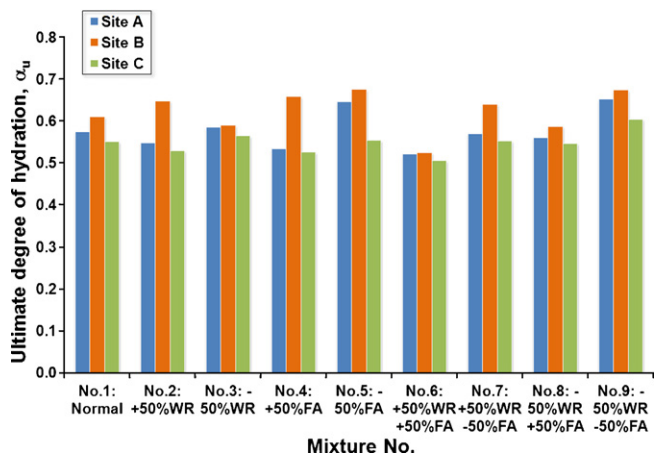

Fig. 7. Calculated α_u from isothermal tests.

Table 4
Hydration curve parameters.

Mixture no.	α_u				β				τ			
	20 °C	30 °C	40 °C	STDEV	20 °C	30 °C	40 °C	STDEV	20 °C	30 °C	40 °C	STDEV
Site A												
No.1: normal	0.606	0.580	0.537	0.035	1.699	1.942	2.242	0.272	18.339	20.823	27.263	4.606
No.2: +50%WR	0.587	0.543	0.515	0.036	1.794	2.295	2.420	0.331	19.154	22.563	27.829	4.371
No.3: −50%WR	0.622	0.601	0.532	0.047	1.622	1.773	2.087	0.237	18.011	18.981	22.566	2.399
No.4: +50%FA	0.542	0.519	0.540	0.013	2.246	2.487	2.311	0.125	20.507	22.933	30.292	5.096
No.5: −50%FA	0.654	0.681	0.603	0.039	1.417	1.773	2.087	0.335	19.154	20.412	26.202	3.759
No.6: +50%WR +50%FA	0.526	0.509	0.529	0.011	2.399	2.670	2.343	0.175	22.161	25.119	32.824	5.505
No.7: +50%WR −50%FA	0.630	0.570	0.510	0.060	1.640	1.922	2.329	0.346	19.546	21.313	24.737	2.639
No.8: −50%WR +50%FA	0.579	0.557	0.543	0.018	1.885	2.199	2.201	0.182	18.157	21.195	27.036	4.513
No.9: −50%WR −50%FA	0.726	0.672	0.558	0.086	1.137	1.337	1.785	0.332	17.849	19.651	20.560	1.380
Site B												
No.1: normal	0.611	0.625	0.596	0.015	2.084	1.721	1.465	0.311	20.247	25.967	29.476	4.659
No.2: +50%WR	0.621	0.662	0.659	0.023	1.729	1.864	1.937	0.105	20.051	29.100	36.721	8.345
No.3: −50%WR	0.591	0.604	0.576	0.014	1.641	1.751	1.937	0.150	20.247	25.967	29.476	4.659
No.4: +50%FA	0.594	0.722	0.660	0.064	1.776	1.668	1.638	0.073	21.749	30.361	34.473	6.494
No.5: −50%FA	0.699	0.722	0.605	0.062	1.361	1.488	1.862	0.260	19.749	24.501	26.943	3.658
No.6: +50%WR +50%FA	0.469	0.499	0.607	0.073	1.641	1.751	1.937	0.150	22.610	29.258	45.811	11.948
No.7: +50%WR −50%FA	0.648	0.664	0.610	0.028	1.557	1.642	2.070	0.275	20.099	23.702	29.178	4.572
No.8: −50%WR +50%FA	0.538	0.605	0.620	0.044	1.808	1.706	1.757	0.051	20.370	24.841	32.634	6.206
No.9: −50%WR −50%FA	0.718	0.696	0.609	0.058	1.245	1.357	1.738	0.259	18.922	20.275	21.612	1.345
Site C												
No.1: normal	0.530	0.491	0.631	0.073	1.606	1.954	1.417	0.272	14.206	16.625	20.419	3.132
No.2: +50%WR	0.501	0.462	0.625	0.085	1.901	2.393	1.547	0.425	16.029	18.339	25.252	4.799
No.3: −50%WR	0.552	0.534	0.607	0.038	1.486	1.685	1.891	0.203	12.975	14.346	25.072	6.624
No.4: +50%FA	0.500	0.462	0.615	0.080	1.636	2.023	1.534	0.258	15.450	16.809	25.164	5.260
No.5: −50%FA	0.506	0.518	0.639	0.074	1.723	1.953	1.471	0.241	14.387	15.017	20.417	3.315
No.6: +50%WR +50%FA	0.471	0.453	0.592	0.075	1.869	2.195	1.730	0.239	17.429	18.374	29.369	6.638
No.7: +50%WR −50%FA	0.535	0.487	0.635	0.076	1.942	2.320	1.716	0.305	15.610	17.105	24.894	4.985
No.8: −50%WR +50%FA	0.519	0.504	0.617	0.062	1.508	1.722	1.368	0.178	14.040	14.724	22.486	4.692
No.9: −50%WR −50%FA	0.603	0.563	0.647	0.042	1.335	1.597	1.372	0.142	11.665	13.246	19.803	4.315

4.3. Hydration curve parameters

The back-calculated hydration curve parameters are presented in Table 4. Results showed that α_u of the same mixtures at different temperatures are close. Theoretically, the ultimate degree of hydration (α_u) would be the same for the same mix given an infinite time for hydration. However, due to the reason that the tests were not continued until the very end of hydration due to test limitation, the same mix resulted in slightly different α_u value. It was also showed that there are no obvious correlations existed between β values and temperatures. However, it was observed that τ value obviously increases with increasing temperature, which indicated a delay of hydration at higher temperature at the same equivalent age (note that not the time), although the heat generation rate is higher at a higher temperature at the same time as discussed previously (see

Figs. 3–5). This is probably due to the fact that at a higher temperature, the equivalent age is higher than that at a lower temperature corresponding to the same time (see Eq. (5)). The mean values of hydration curve parameters were calculated from isothermal tests performed at 20, 30, and 40 °C, the calculated α_u, β, and τ were presented in Figs. 7–9, respectively. Results showed that, in general, α_u (ultimate degree of hydration) decrease with increasing WR dosage and/or FA replacement. As expected, mixture No.6 has the lowest α_u value (9.31%, 14.06%, and 8.23% lower than that of mixture No.1 for the Site A, Site B, and Site C, respectively), while mixture No.9 has the highest α_u value (10.46%, 13.45%, and 9.33% higher than that of mixture No.1 for the Site A, Site B, and Site C, respectively) as shown in Fig. 7. The reduction of amount of WR and FA both resulted in the increase of ultimate DOH.
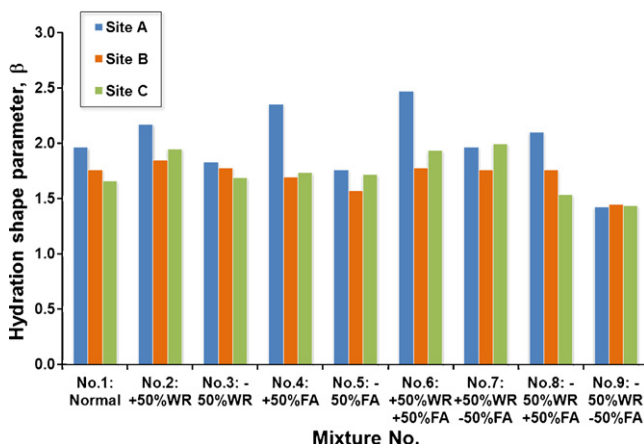

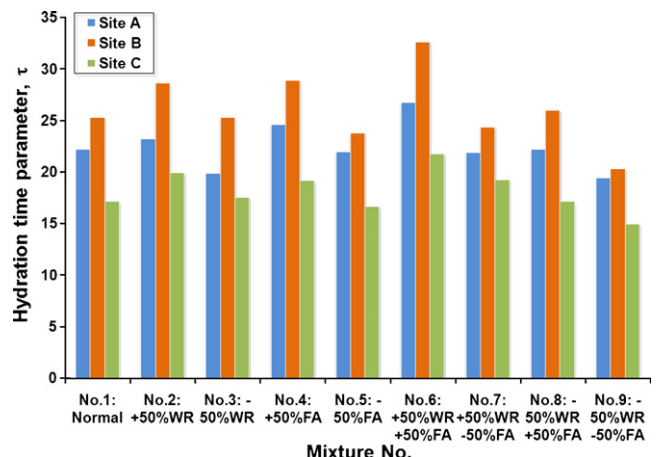**Fig. 8.** Calculated β from isothermal tests.

Fig. 9. Calculated τ from isothermal tests.

Results indicated that the calculated hydration shape parameter β usually increases with increasing WR, and vice versa (i.e. mixture No.2 and No.3 compared to mixture No.1) as shown in Fig. 8. Meanwhile, τ increases with increasing WR and/or FA, that is τ of mixture No.6 are 20.59%, 29.05%, and 27.17% higher than that of mixture No.1 for the Site A, Site B, and Site C, respectively (see Fig. 9). Results were expected since SCMs such as FA generally reduce the overall heat of hydration and particularly the rate of heat liberation, the slow rate of pozzolans reaction in turn resulting in slower heat release [20]. Meanwhile, since all the water reducers used in

the study were also retarder, while the polar lignosulfonate chain adsorbed alongside the cement particle and lowering the surface tension of the water and making the cement particle hydrophilic, the chemical also impede the dissolution of the cement cations and anions and retard the hydration of cement [11,12]. In addition, the early hydration rates of cement chemical compounds were slowed down by extending the length of the induction period [14]. As shown in Figs. 8 and 9, mixture No.9 has the lowest β and τ due to the "coupled" effects of WR and FA. The trend of τ variation is consistent with the activation energy, that is a higher E_a may indicate a larger time delay of hydration. The increase of τ with increasing FA replacement is in agreement with previous research [14].

4.4. Critical temperature and stress developments in early-age concrete pavement

The HIPERPAV® predicted temperature developments in the first 72 h at Site B are shown in Fig. 10. Results showed that while pavement temperature was observed to be significantly affected by the environmental condition, that is, pavement temperature experience daily cycles at the same pace as ambient temperature changes during daytime and nighttime, pavement temperature also changes at different depth inside pavement. It showed that middle point of pavement has the highest temperature, then pavement bottom, and the pavement top has the lowest temperatures due to the heat transfer with the ambient air at the pavement surface while heat conduction with the subbase at the bottom of pavement. Noted that the HIPERPAV® simulations were performed on mixtures from Site A and Site C as well, and the trends very similar to Site B were observed. However, due to the limitation of space, only results from Site B analysis were presented in this paper. Fig. 10 also showed that the pavement temperature decreases by adding FA and/or WR. Mix 6 showed the lowest temperature, while Mix 9 showed the highest temperature. This result is consistent with the hydration parameters discussed previously. The maximum temperature of Mix 6 reduced by 16.16% compared to Mix 1, while the maximum temperature of Mix 9 increased by 4.59% compared to Mix 1. The maximum temperature of Mix 6 was 19.83% lower than that of Mix 1. The temperature differences between mixtures at the earlier age were found to be more significant since the majority of the cement hydration heat was generated within that time period. No significant difference between mixtures was observed later than 48 h after paving, while the ambient temperature instead of heat of hydration started to dominate the changes of pavement temperature.
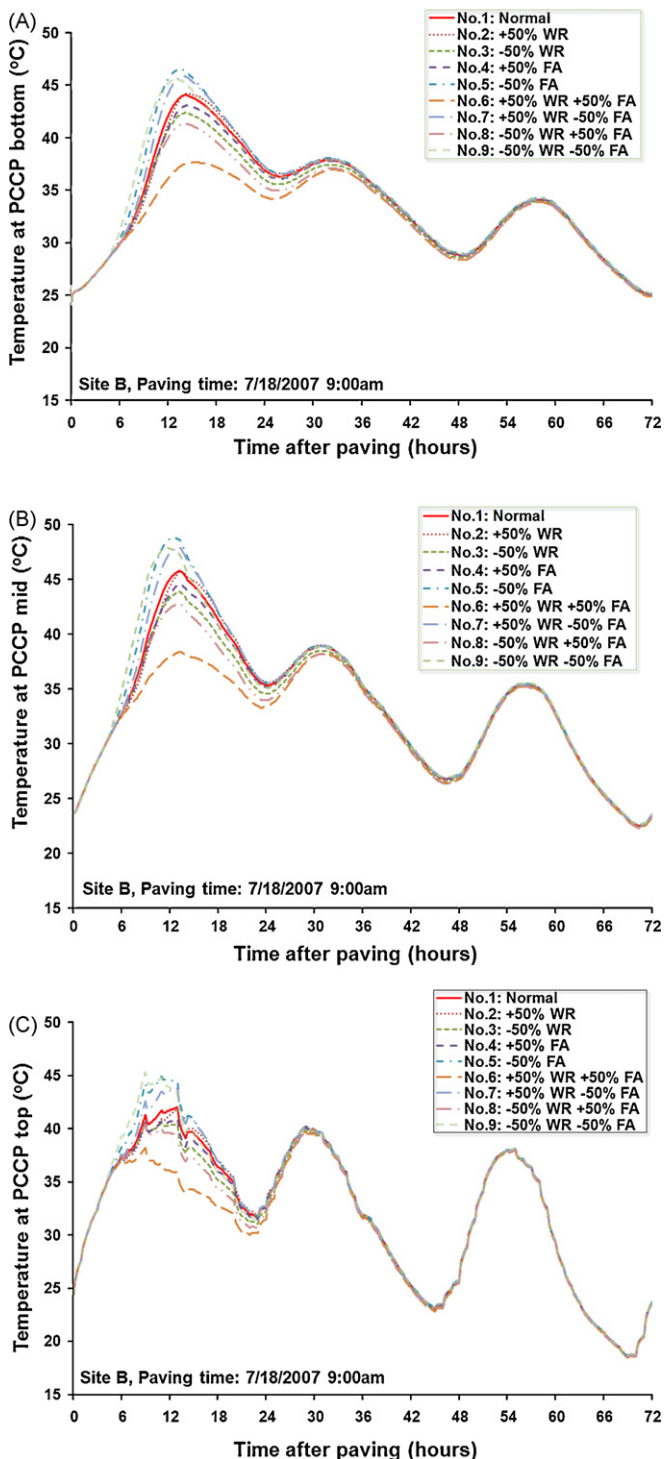

Fig. 10. Predicted temperatures of Site B PCCP.
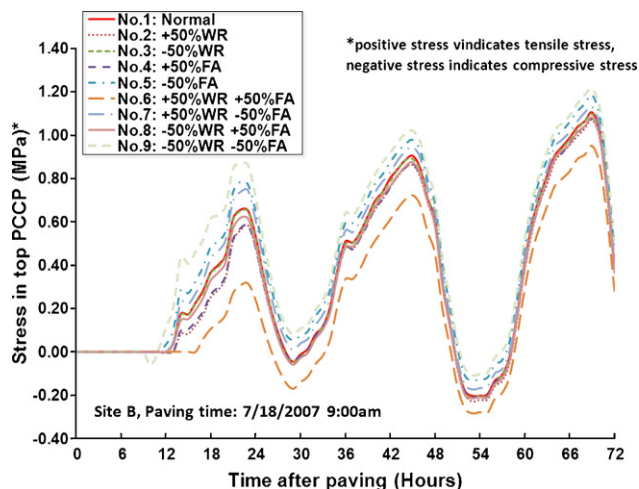

Fig. 11. Predicted tensile stresses of Site B PCCP.

Due to the negative temperature gradient, i.e., lower temperature at the top of PCCP comparing to that at the mid and bottom, the critical tensile stress appears in the top of PCCP. The HIPERPAV® simulation results as shown in Fig. 11 indicated that the calculated tensile stress in top PCCP decreased by adding FA and/or WA, Mix 6 has the lowest stress level, while Mix 9 has the greatest stress level. This result is primarily due to the cement hydration and temperature development discussed above. The tensile stress of Mix 6 reduced by 13.75% compared to Mix 1, while tensile stress of Mix 9 increased by 10% compared to Mix 1. The tensile stress of Mix 9 was found to be 27.54% higher than that of Mix 6. It is noticed that the fly ash and water reducer reduced the development of critical stress due to the delayed hydration process.

5. Conclusions

This paper presented procedures and analyses for ascertaining hydration characteristics from the isothermal calorimetry tests. Study accounted for the influences of water reducer dosage and fly ash replacement on cement hydration. The primary findings and recommendations are summarized as follows:

1. Activation energy E_a mostly increases with increasing water reducer dosage and fly ash replacement.
2. Hydration curve parameters α_u generally decreases, while τ increases with increasing water reducer dosage and fly ash replacement; β generally increases with increasing water reducer dosage.
3. The maximum temperature in the early-age concrete pavement seems to decrease with the increasing water reducer dosage and fly ash replacement, which in turn reduces the thermally-induced critical tensile stress at the top of PCCP.

Acknowledgements

References

[1] W.M. Hale, T.D. Bush, B.W. Russell, S.F. Freyne, Effect of curing temperature on hardened concrete properties, Transp. Res. Rec: J. TRB 1914 (2005) 97–104.
[2] H.T. Yu, L. Khazanovich, M.I. Darter, A. Ardani, Analysis of concrete pavement responses to temperature and wheel loads measured from instrumented slabs, Transp. Res. Rec.: J. TRB 1639 (1998) 94–101.
[3] J.M. Ruiz, A.K. Schindler, R.O. Rasmussen, P.K. Nelson, G.K. Chang, Concrete temperature modeling and strength prediction using maturity concepts in the FHWA HIPERPAV software, in: Proceedings of the 7th International Conference on Concrete Pavements, Orlando, FL, 2001, pp. 9–13.
[4] A.M. Neville, Properties of Concrete, forth ed., Pearson, London, 1995.
[5] T. Nishizawa, T. Fukuda, S. Matsuno, K. Himeno, Curling stress equation for transverse joint edge of a concrete pavement slab based on finite-element method analysis, Transp. Res. Rec.: J. TRB 1525 (1996) 35–43.
[6] A.R. Mohamed, W. Hansen, Effect of nonlinear temperature gradient on curling stress in concrete pavements, Transp. Res. Rec.: J. TRB 1568 (1997) 65–72.
[7] B.F. McCullough, R.O. Rasmussen, Fast-track paving: concrete temperature control and traffic opening criteria for bonded concrete overlays, volume I: final report, FHWA-RD-98-167, FHWA, U. S. Department of Transportation, 1999.
[8] Z. Sun, Q. Xu, Micromechanical analysis of polyacrylamided modified concrete for improving strengths, Mater. Sci. Eng. A: Struct. 36 (2008) 125–127.
[9] Z. Sun, Q. Xu, Microscopic, physical and mechanical analysis of polypropylene fiber reinforced concrete, Mater. Sci. Eng. A: Struct. 527 (2009) 198–204.
[10] A.K. Schindler, K.J. Folliard, Influence of supplementary cementing materials on the heat of hydration of concrete, in: Proceedings of the 9th Conference on Advances in Cement and Concrete, Colorado, August 10–14, 2003.
[11] C. Jolicoeur, M.A. Simard, Chemical admixture–cement interactions: Phenomenology and physic-chemical concepts, Cement Concrete Comp. 20 (1998) 87–101.
[12] L.S. Pan, X.Q. Qiu, Y.X. Pang, D.J. Yang, Effect of water-reducing chemical admixtures on early hydration of cement, Adv. Chem. Res. 20 (2008) 93–100.
[13] J.L. Poole, K.A. Riding, K.J. Folliard, M.C.G. Juenger, A.K. Schindler, Methods for calculating activation energy for portland cement, ACI Mater. J. 104 (2007) 303–311.
[14] A.K. Schindler, Effect of temperature on hydration of cementitious materials, ACI Mater. J. 101 (2004) 72–81.
[15] L. Wadsö, An experimental comparison between isothermal calorimetry, semi adiabatic calorimetry and solution calorimetry for the study of cement hydration, final report, NORDTEST project 1534-01, 2002.
[16] P.F. Hansen, E.J. Pedersen, Maturity computer for controlling. curing and hardening of concrete, Nord. Betong. 9 (1977) 21–25.
[17] J.M. Ruiz, P.K. Kim, A.K. Schindler, R.O. Rasmussen, Validation of HIPERPAV for prediction of early-age jointed concrete pavement behavior, Transp. Res. Rec.: J. TRB 1778 (2001) 17–25.
[18] A.K. Schindler, J.M. Ruiz, R.O. Rasmussen, G.K. Chang, L.G. Wathne, Concrete pavement temperature prediction and case studies with the FHWA HIPERPAV models, Cement Conc. Comp. 26 (2004) 463–471.
[19] V. Rahhal, E. Talero, Influence of two different fly ashes on the hydration of portland cements, J. Therm. Anal. Calorim. 78 (2004) 191–205.
[20] N.Y. Mostafa, P.W. Brown, Heat of hydration of high reactive pozzolans in blended cements: isothermal conduction calorimetry, Thermochim. Acta 435 (2005) 162–167.
[21] R.C. Tank, The rate constant model for strength development of concrete, Ph.D. Dissertation, Polytechnic University, Brooklyn, New York, 1988.